

## Final Technical Report

**Project Title:** The Influence of Radiation on Pit Solution Chemistry as it Pertains to the Transition from Metastable to Stable Pitting in Steels

**Award Number:** DE-FG07-01ER63299

**Award Account:** EMSP 81989

**Period covered** 9/15/2001 – 2/28/2005

**Recipient:** University of Florida  
Chemistry Department  
P.O. Box 117200  
Gainesville, FL 32611

**Principal Investigator:** Prof. Robert Hanrahan  
(352) 392-1441  
[hanrahan@chem.ufl.edu](mailto:hanrahan@chem.ufl.edu)

**In collaboration with:** Dr. R. Scott Lillard  
Los Alamos National Laboratory  
LANL MS G755  
P.O. Box 1663  
Los Alamos, MN 87545-1663

**Project Team:** Dr. Barbara Galuszka-Muga

## NOTICE

**1. Acknowledgment:** This report was prepared as a result of work supported by the U.S. Department of Energy under award No. DE-FG07-01ER63299.

**2. Disclaimer:** Any opinion, findings, and conclusions or recommendations expressed in this material are of those of authors and do not necessarily reflect the views of the Department of Energy.

## Abstract

An investigation was undertaken of the effect of gamma radiation on metastable pitting of mild carbon steels immersed in a solution similar to those existing at high level waste (HLW) deposits in the US. The object was to observe the extent to which a dosage rate of 1 Mrad/hour (10 Kgrey/hour) affected measurable electrochemical parameters such as pitting potential, open circuit potential, rate of metastable pitting and repassivation potential. Methods for reliably measuring electrochemical potentials in a high radiation field were developed. Exploratory analyses were made of the ion product release and electrolyte composition change in a confined volume simulating the conditions of a corrosion initiated pit during gamma irradiation. As expected the results indicated that the metastable pitting rate (as well as the general rate of corrosion) was significantly enhanced by a radiation field.

## Objective

The goal of the UF Radiation Chemistry Group project is to study the effect of gamma radiation on the corrosion of carbon steels (mild steels) under conditions similar to those existing at high level waste (HLW) deposits in the US. The approach involves quantitative electrochemical measurements in a 1 Mrad (10 Kgrey) per hour radiation field of the metastable pitting of steel samples at specified applied potentials as monitored by reference electrodes. In addition, the measurement and analysis is to be made of corrosion product release and electrolyte composition change in micro-volume amounts simulating the environment of actual pitting events.

Key to the implementation of this project was the adaptation of the UF Co-60 irradiator for *in situ* electrochemical measurements. This facility contains 600 curies of Co-60 and is capable of generating a nominal 1.25 MeV gamma ray flux of up to 1 Mrad/hour, depending upon geometry and sample size. During the course of this project considerable innovation was required to meet the challenges of design, development, fabrication, adaptation, reliability, calibration and safely testing of the various components, units and equipment necessary for accurate electrochemical measurements within the irradiator with the Co-60 source lowered in place.

## Methods and Research Approach

### *Miniature reference electrodes*

It was necessary to develop miniature sensor reference electrodes that would be stable over the long time periods in which they were immersed in a high radiation field. Repeated testing of several types and designs of miniature reference electrodes resulted in the use of a custom-built miniature saturated calomel electrode (MSCE). The types of electrodes tested were miniature versions of a (a) Hg/Hg<sub>2</sub>Cl<sub>2</sub> (MSCE), (b) Ag/AgCl(satd) electrode, (c) W/WO<sub>x</sub>(satd KCl) and (d) Cu/Cu<sup>2+</sup>(1 M). Of these, the first two proved to be reasonably stable over weeks of testing in the specified radiation field. Figure 1 is a plot of MSCE vs. Ag/AgCl(satd) over a 7 hour period in a radiation field of 1Mrad/hour. The MSCE was chosen for subsequent experiments; several were fabricated for use and monitored for long term stability. They remained stable over months of intermittent use and stayed within  $\pm 0.5$  mV referenced to a commercially available saturated calomel electrode (SCE). The MSCE (Figure 2) is 3.0 mm in diameter and about 9 cm in length. The electrode container is made from 3.0 mm Pyrex tubing cut to 9 cm length and closed at bottom end. A small aperture is blown out in the side about 2 cm from the closed end and then

closed with a bead of soft glass fused to and thus closing the aperture. On slowly cooling, the soft glass bead will form fine cracks which will allow electrical flow across the bead while precluding liquid flow across the beaded barrier. A second small hole is made near the upper end as a pressure relief pathway. A small drop of liquid mercury is inserted into the bottom using a Pasteur Pipette, commonly called a “spitzer”, fitted with a micro-syringe. Use of a lab jack is advisable to steady the insertion of the pipette tip for delivery. After the mercury drop is deposited on the container bottom, a tenth mL volume of  $\text{Hg}_2\text{Cl}_2$  - saturated KCl slurry can be deposited over the mercury and the tube filled up with saturated KCl solution using the same insertion method. Contact to the mercury drop is made by encasing a 10 cm length of 8 mil (0.2 mm) platinum wire in a small bore glass sheath fused (*i.e.* sealed) at both ends such as to leave approximately 0.5 cm of Pt wire exposed at each end. The glass sheath can be drawn from small bore glass tubing to an outside diameter of about 0.5 mm and cut to the desired length. The top end of the exposed platinum wire is soldered to a small length of multi-strand flexible copper wire and the soldered union is mechanically reinforced by applying heat shrink insulating tubing over the joint. This glass insulated Pt wire with exposed bottom end serves as the mercury contact in the completed reference electrode. Finally, the glass encased Pt wire sheath is inserted into the container to make contact with the Hg pool. A small bead of epoxy can be placed around the top opening to stabilize the assembly mechanically.

#### *Working electrodes*

Thin rectangular shaped metal samples were cut from three types of carbon steels: a) A357CL1, b) A516gr60 and c) A516gr70. Several different versions of encapsulation were used in order to define accurately the exposed surface. The final version was one in which the metal coupon was embedded in a clear epoxy (epofix) hemi-cylindrical casting with insulated electrical contact. The exposed surfaces were ground, polished to a 14000 mesh (less than 1 micron) finish and ultrasonically cleaned before use. Electroplating tape (with cutout) was used to define the exposed surface.

#### *Corrosion Cells*

The design and fabrication of a miniature corrosion cell was also necessary to accommodate the restricted space available in the Co-60 irradiator. Miniature corrosion cells were fabricated from 1.3 cm diameter test tubes and fitted with 3-pin cap connectors. In this way electrical potentials/currents could be monitored inasmuch as each corrosion cell contained a (1) carbon steel coupon as a working electrode, (2) Pt mesh as a counter electrode, and (3) a MSCE (Miniature Saturated Calomel Electrode) as a reference electrode. The electrolyte volume was 5.0 mL. In addition, a larger corrosion cell (50.0 mL electrolyte volume) with fitted cap was fabricated to accommodate the physically larger working electrodes supplied by Los Alamos National Lab (LANL) for a performance comparison test. The electrolyte composition was 0.11 M NaCl/0.19 M NaOH which approximates the alkaline environment in HLW tank solutions. Anions such as nitrates, sulfates and fluorides present in radioactive waste solutions were not included in the electrolyte. Composition of solution simulating Hanford/SRS tank supernatant liquid is shown in Table 1.

Table 1. Composition of solution simulating Hanford/SRS tank supernatant liquid.

Constituent	Concentration (M)
NaNO <sub>2</sub>	1.8
NaNO <sub>3</sub>	3.6
Na <sub>2</sub> HPO <sub>4</sub> ·7H <sub>2</sub> O	0.05
Na <sub>2</sub> SO <sub>4</sub>	0.14
NaAlO <sub>2</sub>	0.57
NaF	0.076
NaCl	0.11
NaOH	0.19

### *Irradiator Cavity Modification*

Renovation of the irradiator cavity was made to accommodate the electrochemical cells as follows:

a) Signal and power cables – Replacement of embrittled feed-through coaxial and power lines was accomplished. Multiple position switch boxes were placed in line for control of four separate corrosion cells.

b) Sample cell holder – A three-position “wagon wheel” sample holder for each type of corrosion cell was fabricated and centered within the irradiator cavity. Strict compliance with radiation safety guidelines was observed during and after the installation of cables and radiation sample holders.

c) Oven and temperature indicator – An insulated, electrically heated oven, monitored with a digital thermometer readout, was built and calibrated for maintaining corrosion cells and their contents at elevated temperatures during the irradiation period.

d) Routine calibration of the Co-60 radiation level was made during the course of this research using the Fricke dosimetry technique<sup>1</sup>.

### *Experimental control, signal processing and recording*

A Gateway 486-66V computer on loan from TOFTEC, Inc. was reconditioned and programmed for control of a PAR/EGG VersaStat unit which was received from LANL. Interfacing a GPIBIIA I/O board and CorrWare/CorrView software installation was completed. Initial experiments using the VersaStat were hampered by oscillations and/or noise in the voltage signals that appeared to increase when the corrosion cell was exposed to radiation. Increasing electrical shielding about the corrosion cell reduced but never quite eliminated this noise.

### *Artificial Pit Assembly*

We have designed an “artificial pit” working electrode in which the starting “pit” volume is about 1 - 2 micro-liter depending on masking dimensions. An exploded view of this assembly is shown in Figure 3 and a front view, after assembly, is shown in Figure 4. In the original proposal the design of the miniaturized corrosion cell did not allow *in situ* optical detection of corrosion products as proposed. A different version the ArtPit (“artificial pit”) was designed and fabricated to study the effect of a limited volume of electrolyte confined in the vicinity of the corroding surface. Component parts of this assembly were cast and fabricated. The “artificial pit” electrode served as the working electrode in the usual three-electrode experimental set-up.

A primary objective of these experiments was to test the effect on pitting of limited (confined) electrolyte volume at the carbon steel surface at different applied potentials (AP), with and without a radiation field at 40°C. In these experiments, the “artificial pit” electrode could be anodically dissolved in a confined volume of electrolyte thus creating a pitting solution similar to that created in a natural pit.

#### *Ion Chromatograph unit*

A Dionex ion chromatograph (IC) unit was purchased at the beginning of second half of project period with the aim of detecting and quantifying metal ions in corrosion products of carbon steels. Elution times have been established for  $\text{Fe}^{+3}$ ,  $\text{Cu}^{+2}$ ,  $\text{Ni}^{+2}$  and  $\text{Mn}^{+2}$  ions and a series of solutions of known dilution was used to establish calibration curves in the concentration range 0.1 to 4.0 ppm.

#### *Cl<sup>-</sup> ion probe measurement*

We have purchased a Lazar ISM-146Cl micro mono ion Chloride electrode referenced to a DJM-146 micro reference electrode and a Jenko Model 6219 microcomputer based PH/mV/ION/TEM meter for  $\text{Cl}^-$  ion determination of small volume samples (0.05 – 0.50 mL) containing  $\text{Cl}^-$  ion concentrations ranging from 1 to 1000 ppm. By measuring the  $\text{Cl}^-$  concentration before and after a electrochemical experiments, we expected to be able to detect the increase of  $\text{Cl}^-$  ions diffusing into the micro-cavity (“artificial pit” region) in response to a concentration gradient which provides counter ions to the dissolved metal ions during the pitting process.

## **Results**

### *Electrochemical noise experiments*

Initial experiments examined the potentiodynamic (PD) scan response as represented in Figures 5 and 6. Figure 6 describes how values of electrochemical parameters such as open circuit potential (OCP), corrosion current density ( $i_{\text{corr}}$ ), passive current density ( $i_{\text{pass}}$ ), pitting potential ( $E_{\text{pit}}$ ) and repassivation potential ( $E_{\text{rp}}$ ) were derived from a typical potentiodynamic polarization curve without hysteresis in the reverse scan. Some general observations made during the course of these investigations were:

- 1) The slower the potentiodynamic (PD) scan rate, the greater the probability that a current excursion will occur. This is true with and without a radiation field.
- 2) The slower the PD scan rate, the smaller is the difference,  $\Delta E$ , between the open circuit potential (OCP) and the repassivation potential ( $E_{\text{rp}}$ ), if  $E_{\text{pit}}$  is not observed.
- 3) In a radiation field and *for fast PD scans* for which a pitting potential  $E_{\text{pit}}$  is not observed as in Figure 5, (a)  $\Delta E$  (OCP- $E_{\text{rp}}$ ) is larger, (b)  $E_{\text{rp}}$  is significantly less negative (larger *re* SCE) and (c) OCP is slightly less negative compared to responses without radiation.
- 4) In a radiation field and *at slow scan rate*, PD scans may produce variations such as (a) multiple OCP values, (b) current excursion (pitting,  $E_{\text{pit}}$ ) at lower voltages, (c) repassivation potential ( $E_{\text{rp}}$ ) value lower than OCP value and (d) possibly no passivation potential ( $E_{\text{rp}}$ ) value at all before terminal voltage is reached. These responses are understood in terms of pitting and crevice induced corrosion but seem to be more intense/frequent/erratic in a radiation environment and attest to the stochastic nature of the pitting process.
- 5) Running PD experiments at elevated temperatures (40°C) gave more consistent results as compared to room temperature (~20°C) experiments.

6) For counter electrodes, a straight Pt wire (0.6 mm diam. x 7.5 cm. length) or Pt wire mesh (0.5 cm x 2.0 cm) was used. No significant difference in behavior was noted.

7) Values of OCP are slightly more negative and  $i_{\text{pass}}$  is larger in a radiation environment. Average values of OCP,  $i_{\text{corr}}$ ,  $i_{\text{pass}}$ ,  $E_{\text{pit}}$  and  $E_{\text{rp}}$  with and without a radiation environment at 40°C are shown in Table 2.

Table 2. Summary of polarization data from A516gr70 samples in 0.11M NaCl / 0.19M NaOH electrolyte at 40°C. Voltages are referenced to a Saturated Calomel Electrode. Current is expressed in amperes/cm<sup>2</sup>. Each data set represents the average of seven separate experiments in a radiation field and six without a radiation environment.

Electrochemical parameters	In Radiation Field	Without Radiation Field
OCP (V)	-0.43 ± 0.05	-0.30 ± 0.03
$i_{\text{corr}}$ (A/cm <sup>2</sup> )	5.2 ± 0.8 x 10 <sup>-7</sup>	1.5 ± 0.5 x 10 <sup>-7</sup>
$i_{\text{pass}}$ (A/cm <sup>2</sup> )	1.7 ± 0.3 x 10 <sup>-6</sup>	4.6 ± 0.8 x 10 <sup>-7</sup>
$E_{\text{pit}}$ (V)	0.41 ± 0.13	0.43 ± 0.05
$E_{\text{rp}}$ (V)	-0.78 ± 0.04	-0.76 ± 0.02

The evolution of metastable pitting events (also referred to as electrochemical noise, EN) can be clearly seen in potentiostatic (PS) holds. Figures 7 and 8 show representative results with, and without an applied radiation field, respectively. During a PS hold, the current is recorded as a function of time, in these cases, data were recorded for a total of 1200 sec. at an acquisition rate of 10 Hz (10 pts./sec). In general for these studies, we used pairs of A516gr70 carbon steel coupons embedded in epoxy resin, run at 40°C, one coupon with and one coupon without a radiation field for comparison. The exposed surface area of working electrode was 0.29 cm<sup>2</sup>. The full experimental cycle was as follows:

- 1) OCP (E vs. time) experiment was recorded for one hour.
- 2) PD scan from -0.10 V (vs. OCP) to 0.0 V (vs. SCE) was followed by two 20-min. PS holds at 0.00 V vs. previous final voltage.
- 3) Sequential PD scans and pairs of 20-min. PS holds were continued in 0.1 V increments until 0.3 V was reached and then 0.02 V increments were applied until 0.5 V was attained. Analysis of potentiostatic holds on pairs of carbon steel samples (with and without applied radiation field) resulted in a proliferation of peaks (pitting events or current excursions), more for irradiated samples, and attests to the enhancement of corrosion by radiation exposure.

Current excursions identified as metastable peaks fall into two categories, short and long duration events. Short duration peaks (SDP) represent passivation events and resemble classical metastable pitting with durations of 1 second or less. Long duration peaks (LDP), sometimes lasting hundreds of seconds, may in fact have short duration peaks superimposed on the broadly based peak. In these cases, the event was analyzed as one broad pitting event. They represent damage events. Peaks corresponding to a charge passed  $\geq 1 \times 10^{-8}$  Coulombs were considered significant and were counted and analyzed. Figures 9 and 10 represent examples of SDP and LDP events, respectively.

Some general observations based on comparison of eight pairs of epoxy embedded samples of A516gr70 include:

- 1) Metastable pitting occurs more frequently in a radiation environment.

2) Metastable pitting tends to begin at lower applied voltages in a radiation environment.  
3) A radiation field tends to produce a larger ratio of SDP/LDP events. This trend suggests that, in a radiation environment, repassivation of the incipient pit is more easily and quickly established.

The metastable pitting events data were plotted as frequency histograms and appear in Figures 11 and 12 in which side-by-side comparison of radiation effects is shown for SDP and LDP events, respectively. These plots represent data analyzed for 16 samples (8 pairs) of carbon steel samples. Clearly, in all cases, the radiation environment results in more pitting. This result is shown again by computing the ratio,  $R_{w/w_0}$ , of events with radiation to events without radiation for SDP and LDP categories. The effect is more pronounced in the case of SDP events. The overall ratio,  $R_{w/w_0}$ , from all charge bins was calculated giving the following results.

- 1) for SDP events  $R_{w/w_0} = 16.7 \pm 6.5$
- 2) for LDP events  $R_{w/w_0} = 3.47 \pm 0.39$

At 1 Mrad/hour dose rate radiation is more effective in initiating both short duration and long duration pits, inasmuch as, in this comparison of the results of many experiments, conditions were identical except for the presence or absence of radiation. On the other hand the ratios

- 3) SDP : LDP in radiation,  $R_{S/L,R} = 0.328 \pm 0.035$
- 4) SDP : LDP w/o radiation,  $R_{S/L,N} = 0.068 \pm 0.027$

indicating that short duration pitting versus long duration pitting is favored in the radiation field by a factor of about five.

### *Artificial Pit Studies*

Preliminary examination of an “artificial pit” assembly reveals that our analytical approach is sufficiently precise to quantify important transition metal ions ( $Fe^{2+}$ ,  $Fe^{3+}$  and  $Mn^{2+}$ ) in small (1 - 2 micro-liter) volume solutions adjacent to the corroding surface. The composition of A516gr70 alloy is: 98.281% Fe, 0.036% Al, 0.230% C, 0.020% Cr, 0.260% Cu, 1.110% Mn, 0.004% Mo, 0.003% Nb, 0.010 Ni, 0.007% P, 0.010% S, 0.260% Si, and 0.019% V. Six experiments (three in a radiation environment and three without radiation) were investigated using ArtPit (Figures 3 and 4) as a working electrode and the alkaline solution (0.11 M NaCl/0.19 M NaOH) as an electrolyte. These experiments were run at elevated temperature of 40°C and the set-up was as follow:

- 1) One hour of OCP (E vs. time) run to stabilize electrode surface.
- 2) Potentiodynamic scan (PD) was run from -0.1 V vs. OCP to 0.4 V vs. SCE followed by eight 40-min. potentiostatic holds (PS) at an applied potential of 0.4 V vs. SCE.

Following the extended PS holds, the ArtPit was removed from electrolyte, rinsed with distilled water and wiped with clean tissue. The ArtPit was carefully disassembled, and each of the opposing surfaces was washed with 5-8 drops of distilled water or ISA (ionic strength adjustor, 0.1 M  $NaNO_3$ ) solution. The latter (ISA solution) was used if  $Cl^-$  was to be analyzed. The rinse solution was collected in 1 cm diameter tared weighing vials and acidified with 1 drop of diluted (0.4 M) sulfuric acid solution for IC analysis. The adjusted rinse volume was determined by gravimetric method just before ion analysis by using a density value of 1 gram/mL. This solution was used for both  $Cl^-$  and  $Fe^{3+}$  ion determination.

Chloride ion analysis was made using a Jenko Model 6219 microcomputer based PH/mV/ION/TEMP meter. The sensing electrode was a Lazar Research Laboratories ISM-146Cl micro mono ion Chloride electrode referenced to a Lazar DJM-146 micro reference

electrode. The system is sensitive in the range 1000 ppm down to 1 ppm  $\text{Cl}^-$  ion. The calibration curve was generated which included the concentrations expected in the test solutions.

Transition metals ( $\text{Fe}^{2+}$ ,  $\text{Fe}^{3+}$ ,  $\text{Mn}^{2+}$ ) ion analysis was made using a Dionex ion chromatograph consisting of a GP50 gradient pump and AD25 absorbance detector. Injection loop volume was 100 microliters (0.1 mL) leading to a IONPAC CG5A (4 x 50 mm) guard column before ion separation in a IONPAC CS5A (4 x 250 mm) analytical column. The eluent used was MetPac PDCA Eluent Concentrate (7.0 mM Pyridine-2,6-dicarboxylic acid (PDCA)/66 mM Potassium hydroxide/5.6 mM Potassium sulfate/74mM Formic acid) diluted 1:5 with distilled water. The eluent flow rate was 2.0 mL/min. The Post Column Regenerate (PCR) was 0.0005 M 4-(2-pyridylazo) resorcinol in MetPac PAR Postcolumn Reagent Diluent (1.0 M 2-Dimethylaminoethanol/0.50 M Ammonium hydroxide/0.30 M Sodium bicarbonate). PCR flow rate was 0.6 mL/min. The resulting metal ion – PAR complex was detected by measuring the absorbance at 530 nm. The calibration curves included concentration ranges from 0.2 to 4 ppm maximum and showed excellent linearity. Ion  $\text{Fe}^{2+}$  did not appear as a separate elution peak as it is rapidly oxidized to  $\text{Fe}^{3+}$  in the alkaline electrolyte as it is generated. Also  $\text{Mn}^{2+}$  ion was not detected in the ArtPit solutions investigated. Figure 13 shows the chromatogram of a standard solution consisting of 0.4 ppm of  $\text{Fe}^{3+}$  and 0.8 ppm of  $\text{Mn}^{2+}$ . Figures 14 and 15 represent chromatograms of solution removed from an “artificial pit” electrode with A516gr70 carbon steel coupon in alkaline solution for a sample being irradiated and non-irradiated, respectively. The second elution peak we attribute to  $\text{Zn}^{2+}$  impurities from an as yet unidentified source.

A summary of the solution analysis of these six ArtPits is detailed in Table 3 for  $\text{Fe}^{3+}$  and  $\text{Cl}^-$  ions. No  $\text{Mn}^{2+}$  was detected although we should have picked up a trace from coupon #5 based on previous work with an exploratory ArtPit experiment. Perhaps this lack of detection is associated with a selectivity in retaining Mn with the bulk metal during the (metastable pitting) dissolution of iron. Another possibility is that the alkaline electrolyte adversely effects the analysis. No particular correlation of analytical data with radiation is evident and reproducibility within each trio is poor except in the values for the  $\text{Fe}^{3+}/\text{Cl}^-$  ratio found for the irradiated trio. We should expect at least a weak correlation between the amount of metal ion detected and the total number of current peaks. This is true for coupon #5, which has largest amount of iron (912 ng) and largest number of peaks (470) while the others seem to have no correlation. Possible causes for this lack of correlation may be:

- 1) diffusion of ions in/out of confined volume during course of experiment,
- 2) failure to recover analytically the small 2  $\mu\text{L}$  ArtPit volume during the rinse cycle or
- 3) random bubbles, gas pockets formed in the ArtPit volume during the prolonged PS holds.

Table 3. Summary of “ArtPit” solution analyses.

Sample No.	Pit Volume (mL)	Con. Fe <sup>3+</sup> (ppm)	Fe <sup>3+</sup> (ng) in pit volume	Con. Cl <sup>-</sup> (ppm)	Cl <sup>-</sup> (μg) in pit volume	Fe <sup>3+</sup> /Cl <sup>-</sup>	Number of pitting events
With radiation							
1	0.00208	0.139	57.4	8.57	2.93	19.5x10 <sup>-3</sup>	206
2	0.00188	0.331	132.0	32.3	6.95	19.0x10 <sup>-3</sup>	71
3	0.00201	0.163	73.2	17.4	3.30	22.2x10 <sup>-3</sup>	7
Without radiation							
4	0.00182	0.846	439.0	10.7	6.01	73.0x10 <sup>-3</sup>	0
5	0.00179	2.16	912.0	4.49	1.59	573.0x10 <sup>-3</sup>	470
6	0.00211	0.0357	17.9	5.11	2.45	7.31x10 <sup>-3</sup>	21

Note: Columns for Fe<sup>3+</sup> and Cl<sup>-</sup> concentrations are recorded data for the rinse solution volumes.

Since these initial experiments were completed, we have established a more efficient and consistent procedure for recovering analytically the contents of the ArtPit confined volume. Experiments now in progress use a neutral NaCl solution as electrolyte. Repetition of these experiments will be made as part of a new grant DE-FG02-05ER64003 which extends the UF portion of this corrosion project.

### Information Access

Currently we are in the process of preparing two publications:

- 1). B. Galuszka-Muga, R.J. Hanrahan, M.A. Hill and R.S. Lillard, “The influence of Gamma Radiation on Pitting Corrosion of Carbon Steels in Alkaline High Level Radioactive Waste Tanks”, to be submitted to *Corrosion*, 2005.
- 2). B. Galuszka-Muga, M.L. Muga and R.J. Hanrahan, “The Effect of Gamma Radiation on the Stability of Miniature Reference Electrodes”.

### References

1. H. Fricke and S. Morse, “The Chemical Action of Roentgen Rays on Dilute Ferrosulfate Solutions as a Measure of Dose”, *Am. J. Roentgenol. Radium Ther.*, **18**, (1927) 426-430.

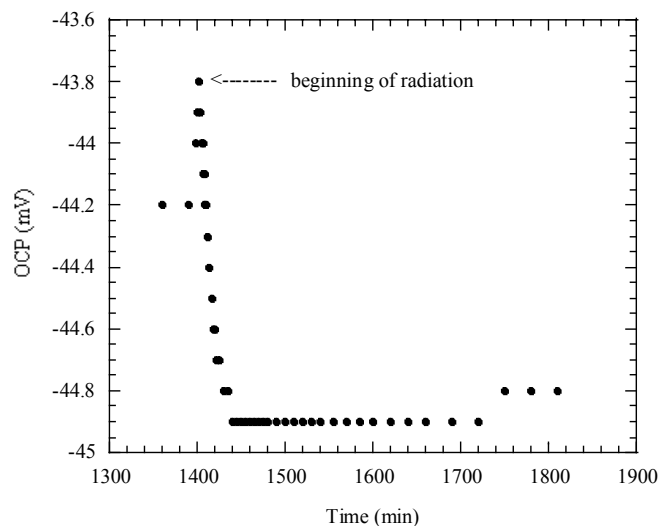


Fig. 1. MSCE vs. Ag/AgCl(satd) exposed to 1 Mrad/hr gamma radiation for 7 hours. The initial variation at beginning of exposure is common to a freshly fabricated electrode system. Variation in voltage may be caused by either electrode.

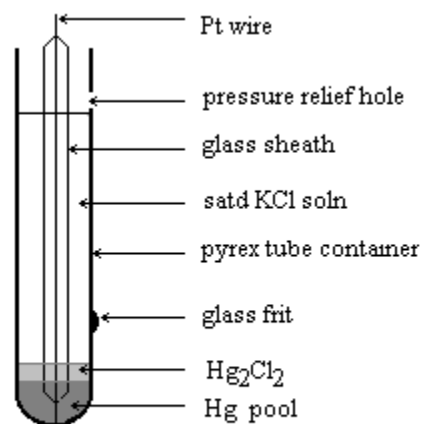


Fig. 2. Miniature Saturated Calomel Electrode (not to scale): height 9 cm, width 3.0 mm. Contact to liquid Hg made by bottom tip of protruding wire insulated in glass sheath.

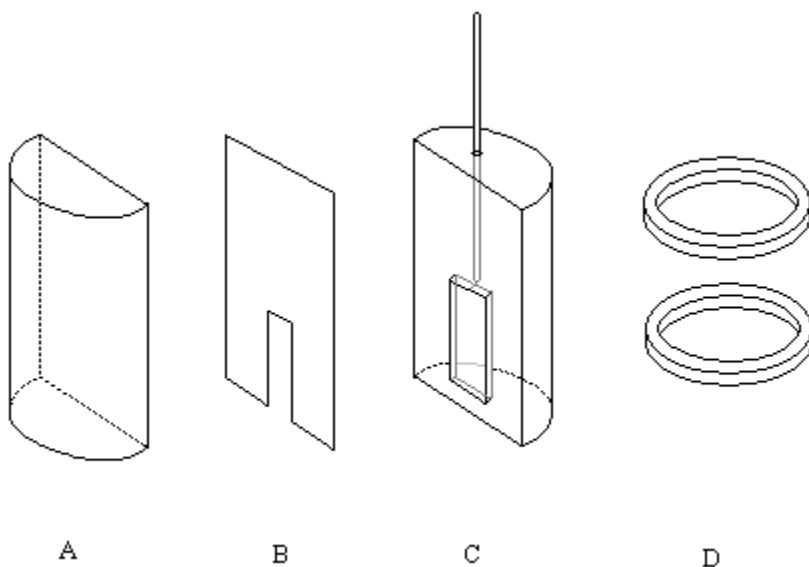


Fig. 3. "Artificial Pit" assembly: slit dimension approximately  $0.3 \text{ cm}^2$ , electroplating tape thickness is  $0.0057 \text{ cm}$ .

A – plastic hemi-cylindrical cover; B – electroplating tape with lower slit applied to coupon; C – plastic hemi-cylinder with embedded coupon and insulated electrical wire attachment through top; D – polyethylene rings for clamping hemi-cylinders together.

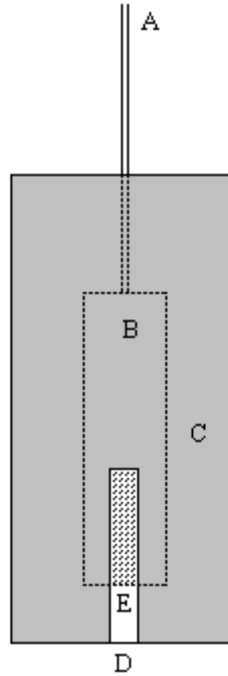


Fig. 4. Front view of working “Artificial Pit” electrode. Coupon embedded in hemi-cylindrical epoxy mold with electroplating tape overlay (dark portion) showing slit and exposed (dotted area) coupon area. A - electrical wire attachment; B – embedded coupon; C- corrosion tape overlay/ mask; D – electrolyte solution access; E – exposed coupon area (dotted area).

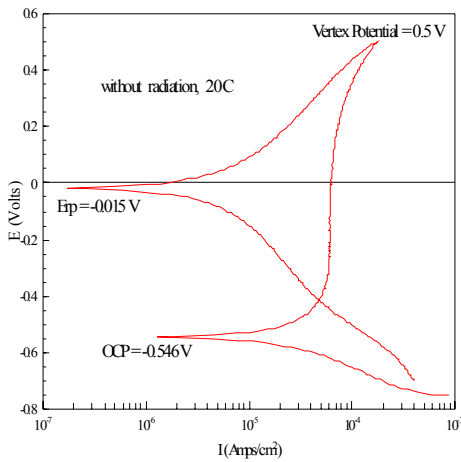


Fig. 5. PD scan for A357CL1 carbon steel sample; scan rate = 5 mV/sec; vertex potential = 0.5 V vs. SCE; without radiation field. Passivating region is almost vertical.

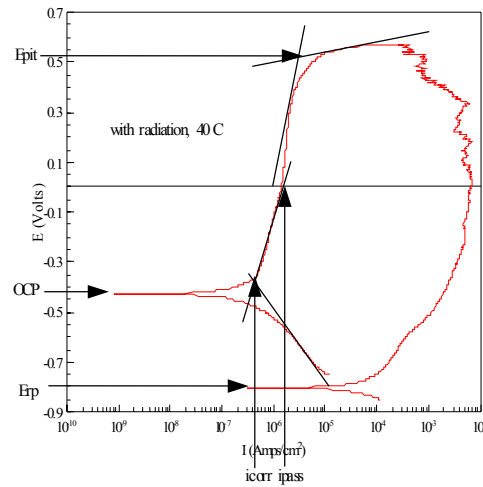


Fig. 6. PD scan for A516gr70 carbon steel sample; scan rate = 0.05 mV/sec; Vertex Potential = 0.6 V vs. SCE; in radiation field. OCP = Open Circuit Potential;  $E_{pit}$  = Pitting Potential;  $E_{rep}$  = Repassivation Potential;  $i_{pass}$  = Passive Current Density;  $i_{corr}$  = Corrosion Current Density.

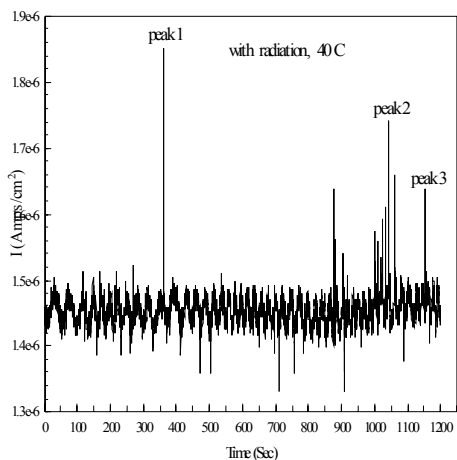


Fig. 7. First 20-min. PS hold at A.P. = 0.423 V vs. SCE for A516gr70 sample in a radiation field.

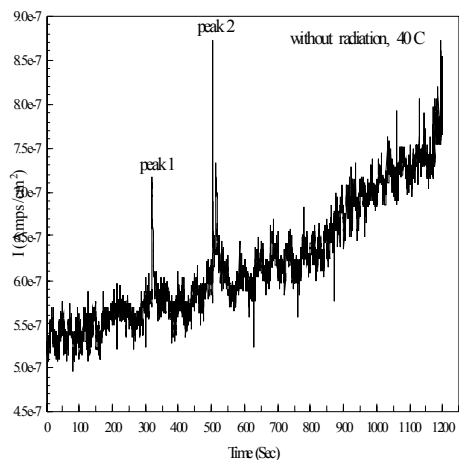


Fig. 8. Second 20-min. PS hold at A.P. = 0.425 V vs. SCE for A516gr70 sample without a radiation field.

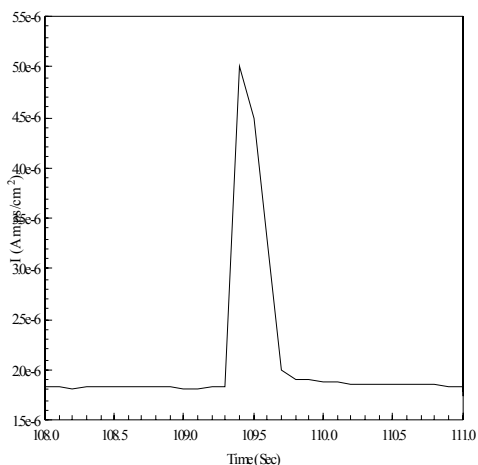


Fig. 9. Current-time transient for A516gr70 sample held at a potential of 0.332 V vs. SCE in a radiation field. The charge passed during the SDP event was  $2.13 \times 10^{-6}$  Coulombs,  $\Delta t = 0.5$  sec.

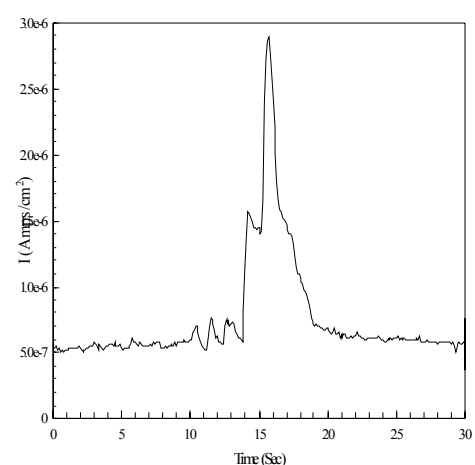


Fig. 10. Current-time transient for A516gr70 sample held at a potential of 0.402 V vs. SCE in a radiation field. The charge passed during the LDP event was  $1.06 \times 10^{-6}$  Coulombs,  $\Delta t = 6.0$  sec.

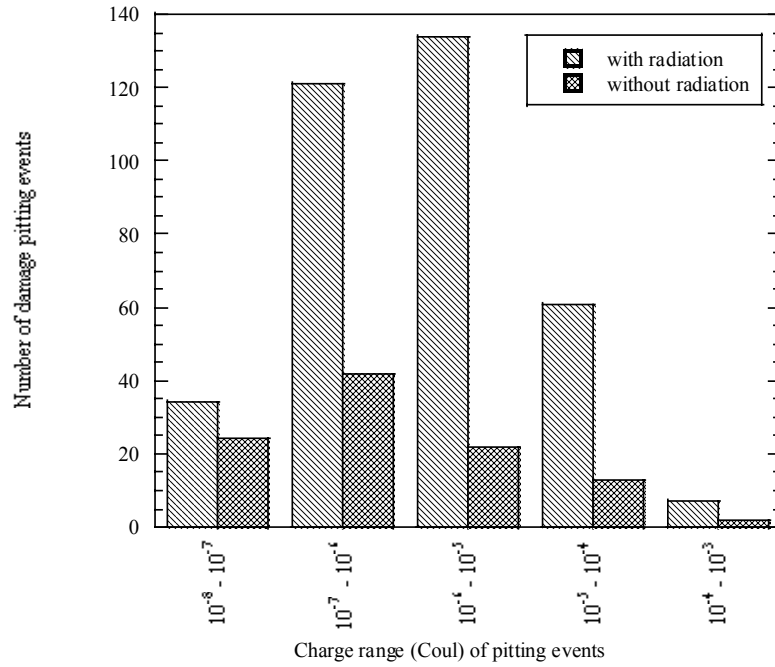


Fig. 11. Histogram representing damage events (LDP) for eight pairs of A516gr70 carbon steel samples in 0.11 M NaCl/0.19 M NaOH solution at 40°C.

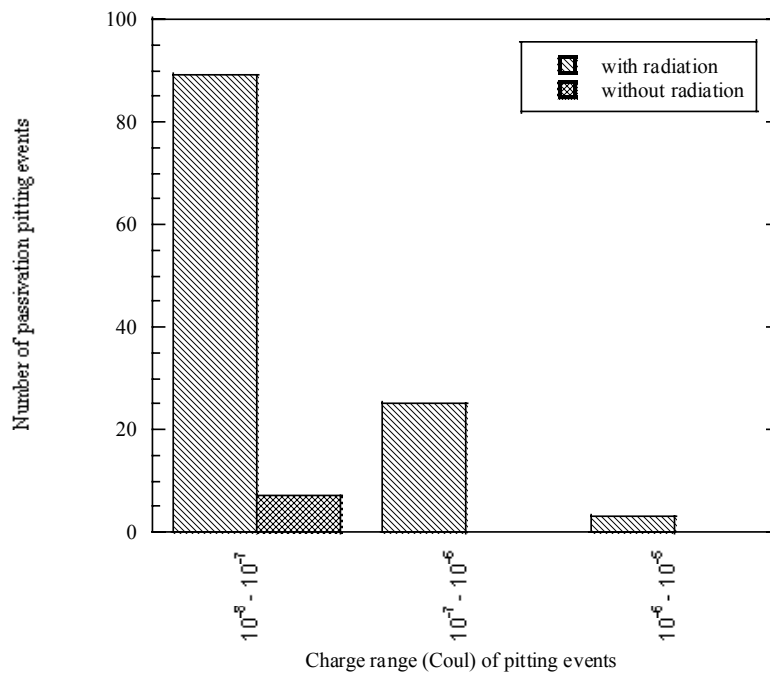


Fig. 12. Histogram representing passivation events (SDP) for eight pairs of A516gr70 carbon steel samples in 0.11 M NaCl/0.19 M NaOH solution at 40°C.

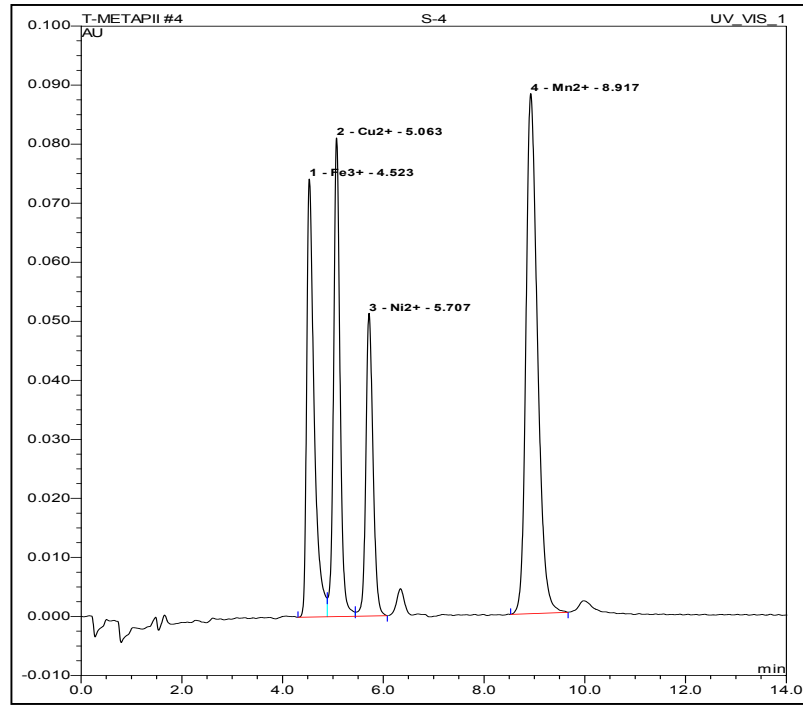


Fig. 13. Chromatogram of a standard solution containing 0.4 ppm of Fe<sup>3+</sup> and 0.8 ppm of Mn<sup>2+</sup>.

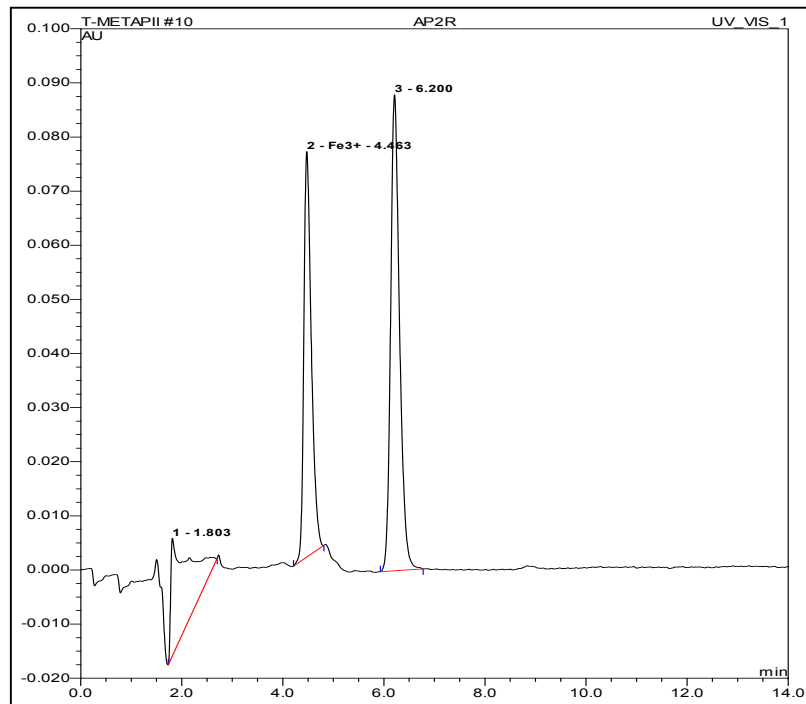


Fig. 14. Chromatogram of solution removed from ArtPit electrode with A516gr70 carbon steel in 0.11 M NaCl/0.19 M NaOH as electrolyte for an irradiated sample.

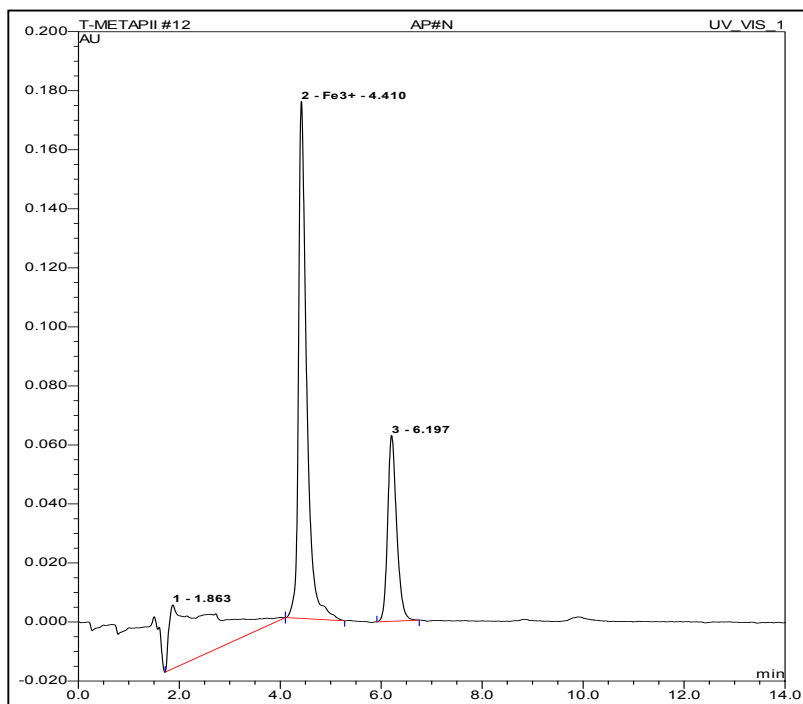


Fig. 15. Chromatogram of solution removed from ArtPit electrode with A516gr70 carbon steel in 0.11 M NaCl/0.19 M NaOH as electrolyte for a non-irradiated sample.

### Acknowledgments

The authors would like to thank the Department of Energy for its support of this project. We would also like to thank Dr. Luis Muga, Professor Emeritus, Chemistry Department, University of Florida, for technical assistance and advice, and Mary Ann Hill of Los Alamos National Laboratory for help in setting up the CorrView control of electrochemical experiments.